JOURNAL OF SOLID STATE CHEMISTRY 6, 519–525 (1973)

The Preparation and Properties of $LaRu_xGa_{1-x}O_3$ Perovskites

R. J. BOUCHARD, J. F. WEIHER, AND J. L. GILLSON

Contribution No. 1869 from the Central Research Department, E. I. du Pont de Nemours and Company, Experimental Station, Wilmington, Delaware 19898

Received May 17, 1972

A series of $LaRu_xGa_{1-x}O_3$ solid solutions was prepared with the orthorhombic $GdFeO_3$-type perovskite structure. Metallic conductivity is observed only for the $LaRuO_3$ end member; the other compounds are semiconductors. Antiferromagnetic interactions and a temperature-dependent magnetic moment are found for Ru^{3+} in this system.

Introduction

We recently examined a new metallic perovskite system, $La_xSr_{1-x}RuO_3$ (*1*), where the Ru valence state decreases continuously from 4+ at $SrRuO_3$ to 3+ at $LaRuO_3$. The magnetic moment/Ru^{3+} in $LaRuO_3$ is anomalously high (2.58 μ_B), and since this is the only example known of Ru^{3+} in an oxide lattice, it is worthwhile to study the variation of magnetic and electrical properties in related systems where the Ru^{3+} concentration becomes more dilute. One possible system is $LaRu_xGa_{1-x}O_3$, where the A ion remains constant and the Ru^{3+} concentration increases from zero to $LaGaO_3$ to 100% in $LaRuO_3$. $LaGaO_3$ has been prepared previously (*2*). It was hoped that perhaps at some critical amount of Ru^{3+} the conductivity would change discontinuously from semiconducting to metallic as a function of temperature.

Experimental

Mixtures of reagent grade oxides were ground in an agate mortar and pestle under N_2 according to the following equation:

$$2La_2O_3 + 2(1-x)Ga_2O_3 + 3xRuO_2 + xRu \rightarrow 4LaRu_xGa_{1-x}O_3.$$

The La_2O_3 was pre-dried at 900°C, stored in a vacuum desiccator and weighed as quickly as possible. The oxide mixtures were pelleted in a hand press, heated to redness in a silica tube under vacuum (to remove any small amounts of H_2O and CO_2 picked up during the grinding and pressing operations), then sealed in evacuated Pt tubes and fired to 1350°C ~ 2 days. The pellets were fairly well sintered and colored black (high Ru content) to brown (low Ru). Standard four-probe resistivity measurements were made and a Faraday balance was used for magnetic data. A Guinier–Hägg camera with KCl as internal standard ($a_0 = 6.2931$Å) and monochromatic Cu$K\alpha$ radiation was used to measure accurate d values, which were refined by a least-squares procedure.

Results

Crystallographic

A complete range of $LaRu_xGa_{1-x}O_3$ solid solutions could be prepared. All compounds have the orthorhombic $GdFeO_3$-type structure D_{2h}^{16}-$Pbnm$, $Z = 4$. The lattice parameters as a function of x are listed in Table I and illustrated in Fig. 1. At ~50% Ru, the unit-cell parameters change from $a > b$ to $a < b$, and in this region, the symmetry is essentially cubic. This behavior is similar to that observed in $La_xSr_{1-x}RuO_3$ (*1*), and in fact, the lattice parameters vs x plots are nearly superimposable. This is somewhat surprising since the A ion is substituted in $La_xSr_{1-x}RuO_3$, and the B ion in $LaRu_xGa_{1-x}O_3$. However, if the B ions are more important in determining the unit cell parameters, then this would be expected because the ionic size differ-

TABLE I

LATTICE PARAMETERS VS COMPOSITION

Formula	a (Å)	b (Å)	c (Å)	V (Å^3)
$LaGaO_3$	5.5223(4)	5.4912(4)	7.772(1)	235.67(2)
$LaRu_{0.1}Ga_{0.9}O_3$	5.5302(7)	5.5009(5)	7.789(1)	236.95(3)
$LaRu_{0.25}Ga_{0.75}O_3$	5.5393(6)	5.5189(5)	7.810(2)	238.77(6)
$LaRu_{0.35}Ga_{0.65}O_3$		~cubic $a_0 = 7.8391(2)$		
$LaRu_{0.5}Ga_{0.5}O_3$	5.5522(3)	5.5551(4)	7.856(1)	242.32(3)
$LaRu_{0.65}Ga_{0.35}O_3$	5.5514(8)	5.6019(6)	7.856(1)	244.32(4)
$LaRu_{0.75}Ga_{0.25}O_3$	5.5466(4)	5.6436(3)	7.8628(6)	246.14(2)
$LaRu_{0.9}Ga_{0.1}O_3$	5.5194(4)	5.7203(4)	7.8545(8)	247.99(3)
$LaRuO_3$	5.4944(6)	5.7789(5)	7.8548(7)	249.40(3)

ence between Ru^{3+} and the other B ion in either solid solution is identical ($Ru^{3+} = 0.68$; Ru^{4+}, $Ga^{3+} = 0.62$ Å).

Electrical

Figure 2 shows resistivity vs temperature for the solid solutions. All are semiconducting except for the end member $LaRuO_3$. There is a fairly monotonic change from semiconducting $LaGaO_3$ to metallic $LaRuO_3$. Figures 3 and 4 and Table II show the smooth variation of room-temperature resistivity and activation energy with x. The activation energies are taken from the straight-line higher-temperature data. $LaGaO_3$ was not measured, but presumably has a gap of at least 3 eV, since it is white.

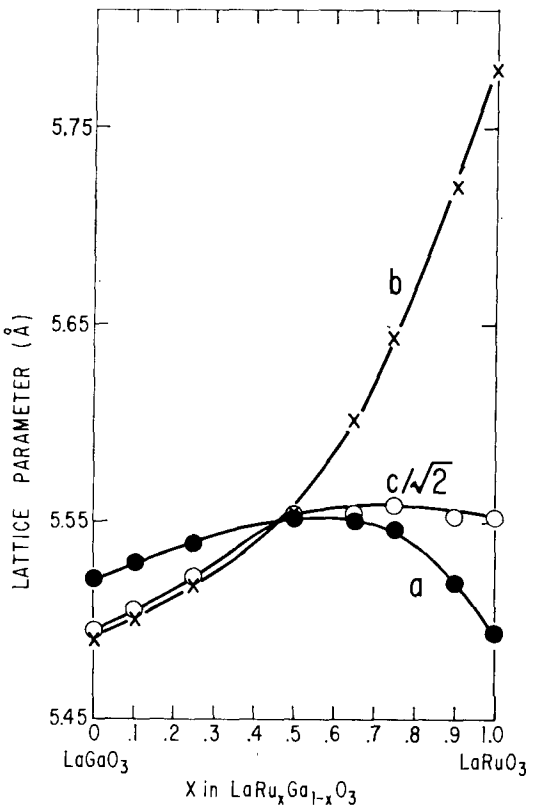

FIG. 1. Lattice parameters as a function of x. $c/\sqrt{2}$ is plotted rather than c since cubic symmetry occurs at $a = b = c/\sqrt{2}$.

Two main features are apparent from the electrical data: (a) no discontinuous behavior or transition occurs for any compound in the temperature range examined; (b) even at 90 mole% Ru, the conductivity is semiconducting, rather than metallic.

All ruthenium perovskites of the type $ARuO_3$ are metallic, presumably because of a partially filled Ru–O π^* band (*3*). Although it would be unrealistic to anticipate a "rigid band" model for the $LaGa_{1-x}RuO_3$ system, i.e., Ru and Ga d orbitals will not overlap, we did expect metallic conductivity at a fairly small concentration of randomly distributed Ru^{3+} ions, perhaps in the 10–20% range, where continuous Ru^{3+}–O–Ru^{3+} interactions could be propagated. We assume that any ordering or clustering is unlikely because Ru^{3+} and Ga^{3+} have the same formal ionic charge and a relatively small ionic size difference. Apparently, however, the electrons are very nearly localized at the Ru^{3+} ions even in $LaRuO_3$, since a small dilution with Ga is enough to disturb the cooperative Ru–O ($t_{2g} - p\pi$) bonding, so that Ru^{3+}–O–Ru^{3+} electron transfer becomes an activated process. The relatively high resistivity of $LaRuO_3$, as noted in the $La_xSr_{1-x}RuO_3$ work (*1*), is consistent with such reasoning.

This tendency toward localization is perhaps not unexpected in view of the behavior of the related perovskites $CaRuO_3$ and $SrRuO_3$. As

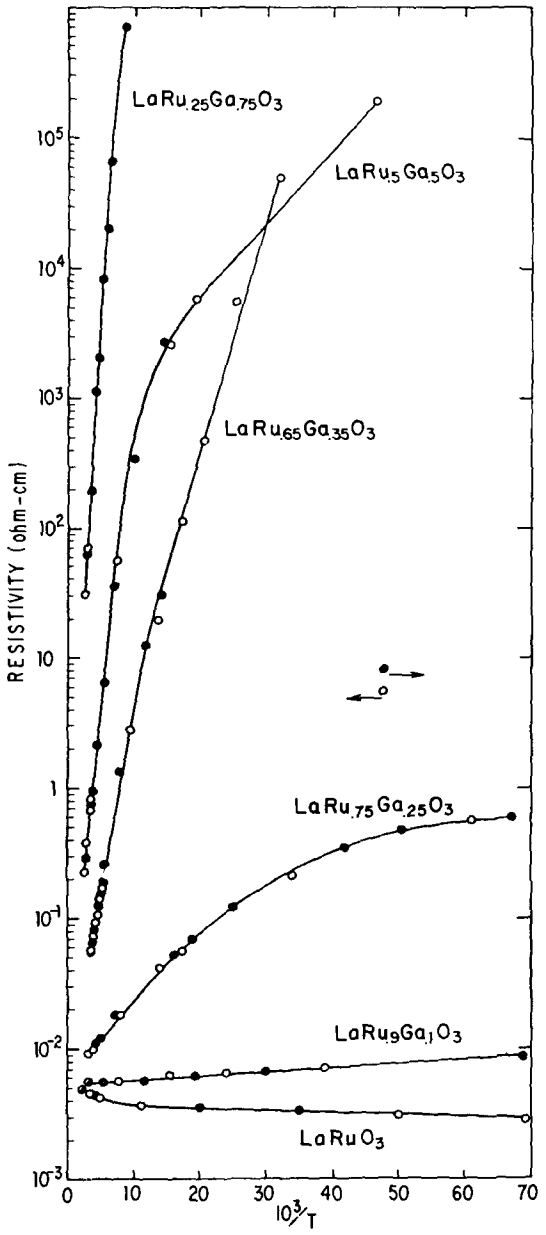

FIG. 2. Resistivity vs temperature for some polycrystalline $LaRu_xGa_{1-x}O_3$ solid solutions.

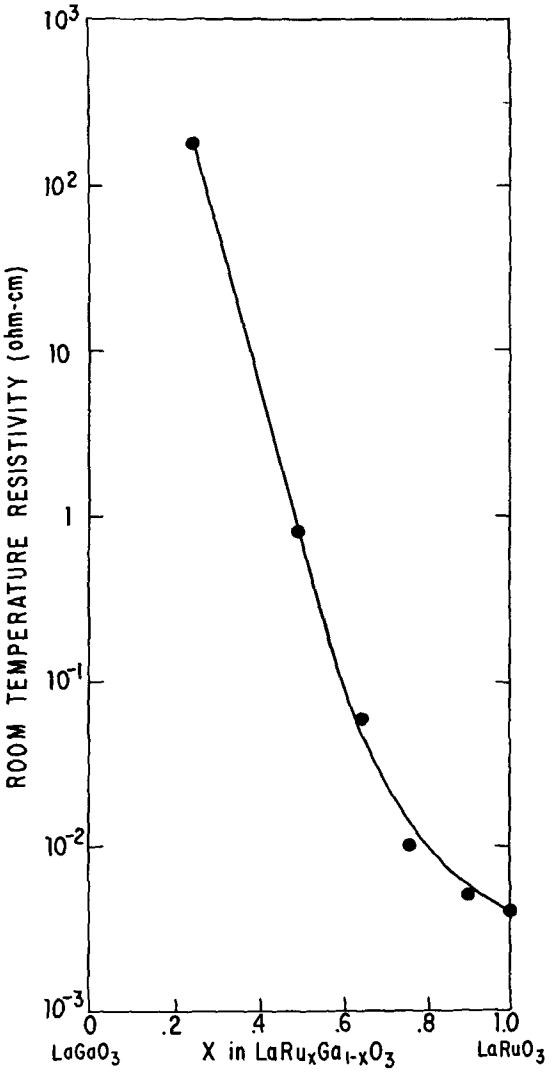

FIG. 3. Room temperature resistivity vs x.

pointed out by Goodenough (*4*), $CaRuO_3$ should have narrower d bands than $SrRuO_3$ because the more acidic, smaller Ca^{2+} competes more strongly for oxide electron density, resulting in weaker Ru^{4+}–O bonding and correspondingly narrower d bands. The La^{3+} ion has about the same size as Ca^{2+}, but its higher positive charge will compete more strongly and narrow the Ru d bands even further, apparently almost to the point of localization. (In fact, for Ru compounds with smaller and more acidic rare earth ions like the $A_2Ru_2O_7$ pyrochlores, semiconductivity is observed (*5*)).

Magnetic

In the $La_xSr_{1-x}RuO_3$ system, the Curie–Weiss θ changed from +160 K at $SrRuO_3$ to −160 K at $LaRuO_3$ (*1*). This was assumed to indicate antiferromagnetic exchange between Ru^{3+} ions in $LaRuO_3$. For $LaGa_{1-x}Ru_xO_3$, therefore, we expected θ to decrease gradually to zero as the Ru concentration decreased. However, extrapolation of the linear, high-temperature portions of the $1/\chi$ vs T plots (Fig. 5) yield substantial negative

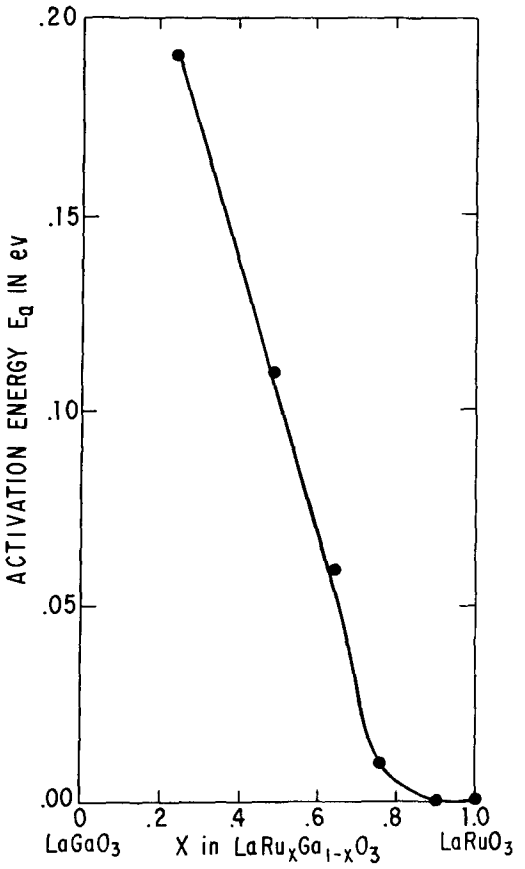

FIG. 4. Activation energy vs x.

θ's for all compositions, even when only 3% Ru is present. Weiss θ's extracted from the data are listed in Table III.

The fact that a large negative θ is exhibited by a composition containing only 3 mole% Ru indicates that antiferromagnetic interactions make only a very small contribution to the θ of $LaRuO_3$.

TABLE II

ROOM-TEMPERATURE RESISTIVITY AND ACTIVATION ENERGY VS COMPOSITION

Formula	Room temperature resistivity (ohm-cm)	Activation energy (eV)
$LaRu_{0,25}Ga_{0,75}O_3$	1.8×10^{2}	0.19
$LaRu_{0,5}Ga_{0,5}O_3$	8×10^{-1}	0.11
$LaRu_{0,65}Ga_{0,35}O_3$	6×10^{-2}	0.06
$LaRu_{0,75}Ga_{0,25}O_3$	1×10^{-2}	0.01
$LaRu_{0,9}Ga_{0,1}O_3$	5×10^{-3}	≈ 0
$LaRuO_3$	—	Metallic

A large *apparent* negative θ can result from a magnetic moment which is temperature-dependent, as is in fact expected for Ru^{3+} (*6*). Since only low-temperature data were available for $LaRuO_3$ (*1*), we measured its susceptibility in the range 300–900 K and this is shown in Fig. 6. The moment calculated from the data, assuming no antiferromagnetic exchange, is plotted vs temperature in Fig. 7(a)—it is strongly temperature-dependent, decreasing rapidly at low temperatures. This behavior is not expected for localized Ru^{3+}, since a low-spin d^5 ground state should exhibit a moment that decreases only moderately at low temperatures, represented by the solid line in Fig. 7(a), plotted from calculations in the literature (*7*).

A moment rapidly decreasing to zero, at 0 K is more reminiscent of Ru^{4+} (d^4) rather than Ru^{3+} (*6*). In fact, a model with localized t_{2g} and itinerant e_g electrons has been proposed for $LaRuO_3$ (*8*). In this model a $t_{2g}^4 e_g^1$ configuration is lower in energy than t_{2g}^5 because of strong intra-atomic exchange correlations—in effect delocalizing one of the Ru t_{2g} electrons into an e_g band. Since this electron would contribute only a small Pauli term, the major term in the susceptibility is from the 4 t_{2g} electrons, analogous to Ru^{4+}.

However, the magnitude of the moment is not consistent with the d^4 interpretation. Providing the temperature region is large enough, the maximum moment in a plot of μ vs $kT/|\lambda|$ (where λ is the spin-coupling constant) peaks at ~3.7 μ_B for d^4 and ~2.5 μ_B for d^5 (*6*). From Fig. 7(a), the effective magnetic moment increases with increasing temperatures to ~2.4 μ_B at 800 K, where it appears to have leveled off. We, therefore, conclude that d^5 is the correct interpretation. Assuming μ_{max} is in the 700–800 K region, the calculated value of λ (from the plot (*6*) of μ vs kT/λ for d^5) is ~1000 K (~700 cm^{-1}), which is considerably lower than the free-ion value for Ru^{3+} (*9*), but not unreasonable when the reduction expected in a covalent oxide lattice is taken into account.

With such strong evidence for a d^5 interpretation provided by the high-temperature moment, we must resolve the apparent discrepancy at low temperatures, namely a moment much lower than calculated theoretically. As previously mentioned however, no antiferromagnetic interactions were assumed in calculating the moments in Fig. 7(a) from the susceptibility data. Most probably, weak antiferromagnetic interactions give rise to

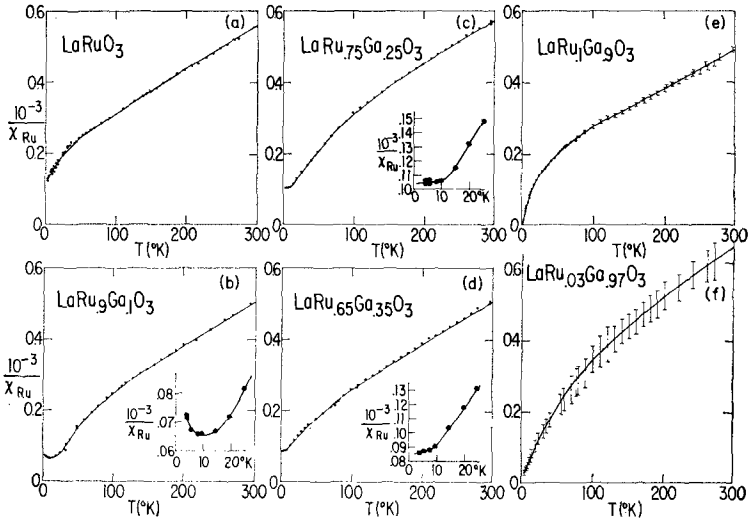

FIG. 5. Inverse magnetic susceptibility per Ru^{3+} vs T as a function of Ru^{3+} concentration. The experimental error in the data is large at (e) and (f) because of the small amount of Ru present.

a small negative θ. In fact, the low-temperature susceptibility data (<30 K) fit to a Curie–Weiss Law yields $\theta \sim -30$ K (Figs. 6 and 5a). This θ raises the calculated moment to ~1.5 μ_B at 0 K and barely affects the high-temperature moment increasing it slighty to ~2.45 μ_B (Fig. 7b). Now the overall temperature dependence of the moment fits well the theory for a t_{2g}^5 system with some delocalization. The calculated curve assumed a spin-orbit coupling constant λ of 695 cm^{-1}, an orbital reduction factor k of 0.9 (a value of $k = 1.0$ corresponds to no delocalization) and no trigonal distortion. The correspondence with the data points is quite good. This agreement with the calculated dependence of μ vs T for all temperatures gives us confidence that the d^5 assignment, with the inclusion of a small negative θ, is valid.

TABLE III

APPARENT θ EXTRAPOLATED FROM HIGH-TEMPERATURE SUSCEPTIBILITY DATA

Ru concentration x	Weiss constant θ (K)
1.00	-160 ± 30
0.90	-110 ± 30
0.75	-160 ± 30
0.65	-110 ± 30
0.10	-160 ± 30
0.03	~ -270

The fit obtained using an orbital reduction factor k of 0.9 emphasizes the low spin-orbit coupling constant of 695 cm^{-1}, since normally the one electron spin-orbit coupling constant ζ ($\lambda = \zeta/2S$) is approximated by $k\zeta_0$, and 695 cm^{-1} is much lower than 0.9 (1180 cm^{-1}), where 1180 cm^{-1} is the free-ion value for Ru^{3+} (*9*). However, the free ion ζ for Ru^0 is 745 cm^{-1} (*10*). This suggests that the total effective *charge* distribution at the Ru in $LaRuO_3$ is closer to Ru^0 than Ru^{3+}. This is not unexpected in view of the strong Ru–O σ-bonding utilizing Ru e_g orbitals, which would tend to decrease the charge distribution around the Ru by partial O → Ru charge transfer. In fact, in his ReO_3 band structure calculation, Mattheiss (*11*) found a charge density corresponding to approximately Re^{3+}, not Re^{6+}.

For very dilute Ru^{3+} compositions, the *low-temperature* susceptibility (Figs. 5e and f) indicate that θ is much smaller or even zero. This is the expected behavior if θ is due to interatomic Ru–Ru interactions. Thus the *apparent* Curie–Weiss behavior of the $1/\chi$ vs T plots in the high-temperature region (Table III) for these and similar compounds must be regarded as a fortuitous result of an intrinsic temperature-dependent moment. Hence, the θ derived from low-temperature data reflect *inter*atomic interactions, whereas the apparent θ from high-temperature data reflects *intra*atomic interactions. Since this was not realized when the $La_xSr_{1-x}RuO_3$ work was

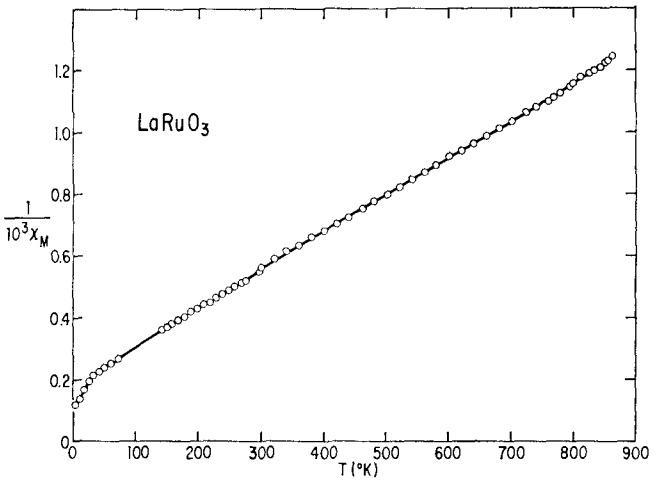

FIG. 6. Inverse magnetic susceptibility vs T for $LaRuO_3$.

published (*1*), the θ values reported there are undoubtedly too negative (and the moments too large) on the La-rich end of the series. However, the change in the sign of the interaction with La substitution into $SrRuO_3$, i.e., from ferro- to antiferromagnetic, is unambiguous.

The effective moments at room temperature for the $LaRu_xGa_{1-x}O_3$ solid solutions are listed in Table IV. Not counting the 3% Ru sample, the rest of the compounds have a moment of 2.12 ± 0.08 μ_B. No particular trend is observed, and for our purposes, the Ru moment can be considered essentially independent of composition.

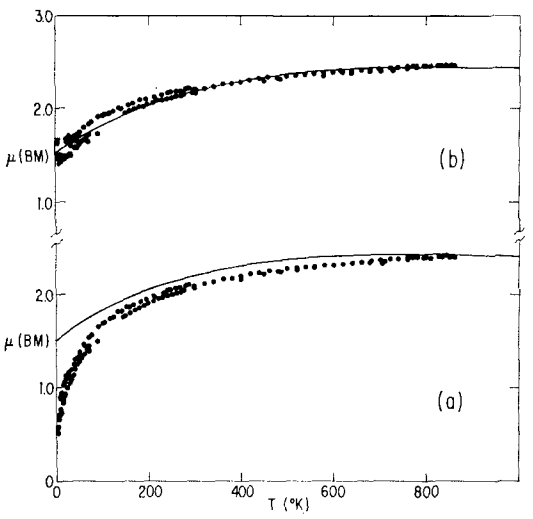

FIG. 7. Magnetic moment μ_{eff} vs T for $LaRuO_3$. In (a), no θ has been included in the μ_{eff} calculation. In (b), a θ of −30 K was assumed (see text). The solid line is the calculated moment for a d^5 system assuming no trigonal distortion, spin-orbit coupling constant $\lambda = 695$ cm^{-1}, and orbital reduction factor $k = 0.9$.

Note for intermediate Ru^{3+} concentrations (Figs. 5b–d), the low-temperature behavior of the susceptibility is characteristic of antiferromagnetic ordering. Pure $LaRuO_3$ (Fig. 5a), however, is different in that no minimum in $1/\chi$ vs T plot is observed down to 4.2 K. For extremely dilute Ru^{3+} concentrations, no evidence for ordering is present either (Figs. 5e, f). This suggests that the total Ru–Ru interatomic interactions are greatest at intermediate concentrations. How might this occur?

If the unit cells of the solid solution remained identical as Ga^{3+} is substituted for Ru^{3+}, the total antiferromagnetic interactions should de-

TABLE IV

THE MAGNETIC SUSCEPTIBILITY AND μ_{eff} AT ROOM TEMPERATURE (RT) VS x[a]

x in $LaRu_xGa_{1-x}O_3$	$10^3\,\chi_{Ru}(RT)$	$\mu_{eff}\,(RT)$
1.0	1.76 ± 0.05	2.04 ± 0.03
0.90	1.93 ± 0.06	2.13 ± 0.03
0.75	1.76 ± 0.01	2.04 ± 0.01
0.65	2.02 ± 0.03	2.19 ± 0.02
0.10	2.04 ± 0.03	2.20 ± 0.02
0.03	1.4 ± 0.4	1.85 ± 0.26

[a] The values given are averages of at least two susceptibility runs.

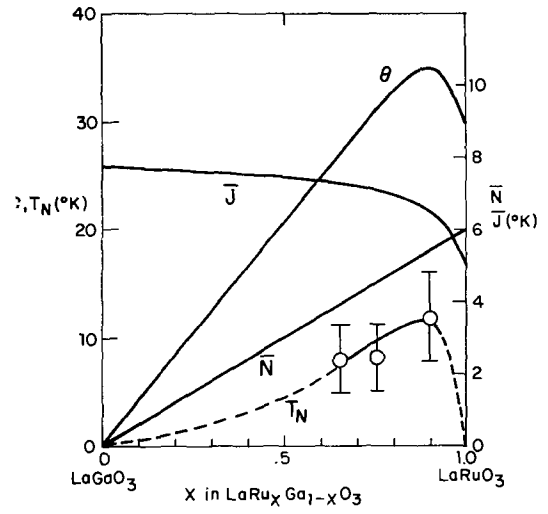

FIG. 8. The qualitative dependence of θ vs increasing Ru^{3+} concentration, assuming a decreasing average Ru–Ru interaction ($\bar{J}_{Ru-Ru}$) which decreases especially rapidly near $LaRuO_3$ because of lattice parameter changes, and an increasing average number of Ru nearest neighbors ($\bar{N}$). T_N values are included for those compositions where a well-defined minimum or discontinuity could be observed in the inverse susceptibility vs T plots.

crease monotonically since the number of nearest-neighbor Ru^{3+} ions around a given Ru decreases linearly, assuming statistical distribution. However, the lattice is contracting with increasing Ga^{3+}, and moreover is changing rapidly as Ga^{3+} is first introduced (Fig. 1); the b axis drops dramatically and the overall symmetry becomes cubic at ~50% Ga. Thus the effective interaction per Ru–Ru pair ought to also be affected, probably strongly. Therefore, two effects must be considered: (1) dilution of Ru^{3+} and (2) contraction and anomalous large changes in the lattice at the Ru^{3+}-rich end of the solid solution series. If the decrease in overall interactions due to the dilution effect is overtaken by the increase due to lattice contractions, a maximum in these interactions would be expected at intermediate concentrations. This is schematically shown in Fig. 8. Although θ is directly proportional to the product of $\bar{J}$ and $\bar{N}$, T_N is much more complicated since it is so sensitive to symmetry and the details of $\bar{J}$. Nevertheless, the T_N's are put in the figure and they do seem to roughly parallel the behavior of θ.

Acknowledgments

We would like to thank H. S. Jarrett and W. Bindloss for helpful discussions.

References

1. R. J. BOUCHARD AND J. F. WEIHER, *J. Solid State Chem.* **4**, 80 (1972).
2. S. GELLER, *Acta Crystallogr.* **10**, 243 (1957).
3. J. B. GOODENOUGH, *Bull. Soc. Chim. Fr.* **1965**, 1200.
4. J. M. LONGO, P. M. RACCAH, AND J. B. GOODENOUGH, *J. Appl. Phys.* **39**, 1327 (1968).
5. R. J. BOUCHARD AND J. L. GILLSON, *Mater. Res. Bull.* **6**, 669 (1971).
6. B. FIGGIS, *J. Inorg. Nucl. Chem.* **8**, 476 (1958).
7. B. N. FIGGIS, *Trans. Faraday Soc.* **57**, 198 (1961).
8. J. B. GOODENOUGH, *Mater. Res. Bull.* **6**, 967 (1971).
9. M. BLUME, A. J. FREEMAN, AND R. E. WATSON, *Phys. Rev.* **134**, A320 (1964).
10. T. N. DUNN, *Trans. Faraday Soc.* **57**, 1441 (1961).
11. L. F. MATTHEISS, *Phys. Rev.* **181**, 987 (1969).